Human Molecular Genetics, 2012, Vol. 21, No. 5 **1111–1123**
doi:10.1093/hmg/ddr540
Advance Access published on November 17, 2011

C/EBPβ and RUNX2 cooperate to degrade cartilage with MMP-13 as the target and HIF-2α as the inducer in chondrocytes

Makoto Hirata[1,2,*], Fumitaka Kugimiya[1], Atsushi Fukai[1], Taku Saito[1,3], Fumiko Yano[2], Toshiyuki Ikeda[3], Akihiko Mabuchi[4], Bishwa Raj Sapkota[4], Toru Akune[5], Nao Nishida[4], Noriko Yoshimura[5], Takumi Nakagawa[1], Katsushi Tokunaga[4], Kozo Nakamura[1], Ung-il Chung[2] and Hiroshi Kawaguchi[1]

[1]Sensory and Motor System Medicine, [2]Center for Disease Biology and Integrative Medicine, [3]Bone and Cartilage Regenerative Medicine, [4]Department of Human Genetics and [5]22nd Century Medical and Research Center, Faculty of Medicine, University of Tokyo, Hongo 7-3-1, Bunkyo-ku, Tokyo 113-8655, Japan

Received August 19, 2011; Revised October 24, 2011; Accepted November 14, 2011

To elucidate the molecular mechanism underlying the endochondral ossification process during the skeletal growth and osteoarthritis (OA) development, we examined the signal network around CCAAT/enhancer-binding protein-β (C/EBPβ, encoded by *CEBPB*), a potent regulator of this process. Computational predictions and a C/EBP motif-reporter assay identified RUNX2 as the most potent transcriptional partner of C/EBPβ in chondrocytes. C/EBPβ and RUNX2 were induced and co-localized in highly differentiated chondrocytes during the skeletal growth and OA development of mice and humans. The compound knockout of *Cebpb* and *Runx2* in mice caused growth retardation and resistance to OA with decreases in cartilage degradation and matrix metalloproteinase-13 (Mmp-13) expression. C/EBPβ and RUNX2 cooperatively enhanced promoter activity of *MMP13* through specific binding to a C/EBP-binding motif and an osteoblast-specific *cis*-acting element 2 motif as a protein complex. Human genetic studies failed to show the association of human *CEBPB* gene polymorphisms with knee OA, nor was there a genetic variation around the identified responsive region in the human *MMP13* promoter. However, hypoxia-inducible factor-2α (HIF-2α), a functional and genetic regulator of knee OA through promoting endochondral ossification, was identified as a potent and functional inducer of C/EBPβ expression in chondrocytes by the *CEBPB* promoter assay. Hence, C/EBPβ and RUNX2, with MMP-13 as the target and HIF-2α as the inducer, control cartilage degradation. This molecular network in chondrocytes may represent a therapeutic target for OA.

INTRODUCTION

The endochondral ossification process plays a crucial role in normal skeletal growth (1) and development of osteoarthritis (OA) which is one of the most common joint disorders today (2–7). This process starts with hypertrophic differentiation of chondrocytes expressing type X collagen (COL10A1), followed by cartilage degradation by proteinases like matrix metalloproteinases (MMPs) and a disintegrin and metalloproteinase with thrombospondin type-1 motifs (ADAMTSs) (8,9). Aiming at elucidation of the molecular mechanism underlying endochondral ossification and identification of therapeutic targets for OA, we previously established a comprehensive screening system of transcription factors that induce chondrocyte hypertrophy using a universal enhancer in the promoter of human *COL10A1* gene as the reporter construct (10), and identified CCAAT/enhancer-binding protein-β (C/EBPβ, encoded by *CEBPB*) as one of the strongest transactivators in chondrocytes (11). C/EBPβ, a member of the leucine zipper family of transcription factors, regulates expression of various genes involved in cell differentiation, proliferation, survival, immune function, female reproduction

*To whom correspondence should be addressed. Tel: +81 338155411; Fax: +81 338184082; Email: hiratam-tky@umin.ac.jp

and tumor progression (12,13). Recent studies by others and us have demonstrated that C/EBPβ plays a role in the endochondral ossification process, since the knockout (*Cebpb*$^{-/-}$) mice exhibit growth retardation probably due to impaired hypertrophic differentiation of chondrocytes (11,14,15). However, the growth retardation is mild and temporary for a limited period during embryogenesis, and disappears after birth. We have therefore hypothesized that C/EBPβ is one of the players in a capital molecular network for the endochondral ossification process, and have sought to identify its transcriptional partners, target molecules and upstream signals in chondrocytes during the skeletal growth and OA development.

RESULTS

RUNX2 is identified as a transcriptional partner of C/EBPβ in chondrocytes

To identify transcriptional partners that enhance transactivity of C/EBPβ, we initially performed a screening using an *in silico* database of protein interactions (STRING), and predicted 178 genes with confidence scores of ≥0.7 as functional partners of human C/EBPβ protein (Supplementary Material, Table S1). Among the genes, we selected 14 genes that satisfied the three criteria: (i) being selected by two or more methods out of seven in the STRING, (ii) transcription factors and (iii) being expressed in chondrocytes (Supplementary Material, Fig. S1). We then performed the second screening of transcription factors using human chondrogenic SW1353 cells co-transfected with a reporter construct containing three consensus C/EBP-binding sequences and expression vectors of the 14 genes selected in the first screening. To exclude the effects of other endogenous C/EBP proteins, we created stable cell lines retrovirally transfected with *CEBPB* gene or the small interfering RNA (siRNA) specific for *CEBPB*. Among the 14 genes, runt-related transcription factor 2 (RUNX2) and activating transcription factor 4 (ATF4) most strongly induced the transactivity of the baseline (*GFP* or si*GFP*-transfected cells) (Fig. 1A). Although the *CEBPB* overexpression further enhanced the transactivities of both RUNX2 and ATF4, the *CEBPB* knockdown significantly suppressed only RUNX2 transactivity, indicating that RUNX2 is the most potent transcriptional partner of C/EBPβ in chondrocytes. Mammalian two-hybrid assay by transfections of vectors expressing GAL4–RUNX2 and VP16–C/EBPβ fusion proteins with the luciferase reporter vector with GAL4-binding sites into HeLa cells showed the molecular interaction between C/EBPβ and RUNX2 (Fig. 1B).

When we compared expression patterns of C/EBPβ and RUNX2 in cultures of mouse primary chondrocytes, mouse chondrogenic ATDC5 cells and SW1353 cells, both expressions similarly increased according to differentiation of all cells (Fig. 1C). In the growth plate cartilage of adult mice, C/EBPβ and Runx2 were co-localized in highly differentiated chondrocytes of hypertrophic and later differentiation stages during expression of Col10a1 and Mmp-13 (Fig. 1D). Subcellularly, C/EBPβ and RUNX2 were co-localized inside the nucleus, especially at the nuclear speckles including active transcription sites (Fig. 1E).

C/EBPβ and RUNX2 cooperatively control skeletal growth

To determine the involvement of C/EBPβ and RUNX2 in the skeletal growth, we generated their compound-knockout mice by appropriate mating. Because the *Runx2* homozygous-knockout (*Runx2*$^{-/-}$) mice died just after birth, we used the heterozygous-knockout (*Runx2*$^{+/-}$) mice. *Cebpb*$^{-/-}$ and *Cebpb*$^{-/-}$;*Runx2*$^{+/-}$ mice were born at much lower frequencies than the expected Mendelian ratio and short-lived even after birth. Although *Cebpb*$^{+/-}$ mice were normal, *Cebpb*$^{-/-}$ mice exhibited mild and temporary dwarfism only for a limited period during embryogenesis, and grew normally after birth, as we previously reported (11). *Runx2*$^{+/-}$ and *Cebpb*$^{+/-}$;*Runx2*$^{+/-}$ mice did not show a significant growth retardation; however, *Cebpb*$^{-/-}$;*Runx2*$^{+/-}$ mice showed more severe dwarfism than their *Cebpb*$^{-/-}$ littermates during the perinatal periods (Fig. 2A and Supplementary Material, Fig. S2A) and remained smaller than the other genotype littermates even 12 weeks after birth (Fig. 2B). Cleidocranial dysplasia with hypoplastic clavicle and open fontanelle were also enhanced by the compound insufficiency (Fig. 2A and Supplementary Material, Fig. S2B and C). The percentage of the proliferative zone relative to the total limb length was increased in *Cebpb*$^{-/-}$, *Cebpb*$^{+/-}$;*Runx2*$^{+/-}$ and *Cebpb*$^{-/-}$;*Runx2*$^{+/-}$ littermates, indicating a delay of chondrocyte hypertrophy by the *Cebpb* insufficiency (Fig. 2C and D and Supplementary Material, Fig. S3A and B), as previously reported (11,14). The percentage of the proliferative zone and the start of chondrocyte hypertrophy were similar between *Cebpb*$^{-/-}$ and *Cebpb*$^{-/-}$;*Runx2*$^{+/-}$ littermates; however, that of the hypertrophic zone with Col10a1 expression was elongated and that of the bone area was markedly decreased in the *Cebpb*$^{-/-}$;*Runx2*$^{+/-}$ limbs (Fig. 2C–E and Supplementary Material, Fig. S3A and B), demonstrating that *Runx2* insufficiency caused impairment of steps later than chondrocyte hypertrophy under the *Cebpb* deficiency. Since this impairment was associated with a decrease in Mmp-13 expression, C/EBPβ and RUNX2 seem to cooperatively promote matrix degradation through the Mmp-13 induction (Fig. 2E and Supplementary Material, Fig. S4). Although the Mmp-3 expression was also considerably decreased in the *Cebpb*$^{-/-}$;*Runx2*$^{+/-}$ limbs, this may be due to the effect of deficiency of both alleles of *Cebpb* because it was similarly decreased in the *Cebpb*$^{-/-}$ limbs (Supplementary Material, Fig. S4). Expressions of other proteinases like Mmp-9, Adamts4 and Adamts5, as well as vascular endothelial growth factor (Vegf), an essential protein for vascularity, were little affected by the *Cebpb* or *Runx2* insufficiency (Supplementary Material, Fig. S4). When we examined the histological phenotypes of the compound deficient mice after birth, the hypertrophic zone seemed to have gradually been restored to normal, and by 16 weeks of age the growth plate phenotype in *Cebpb*$^{-/-}$;*Runx2*$^{+/-}$ mice was ameliorated (Supplementary Material, Fig. S3A–C).

C/EBPβ and RUNX2 cooperatively control OA development

In addition to the physiological role in the skeletal growth, we next examined the contribution of C/EBPβ and RUNX2 to OA

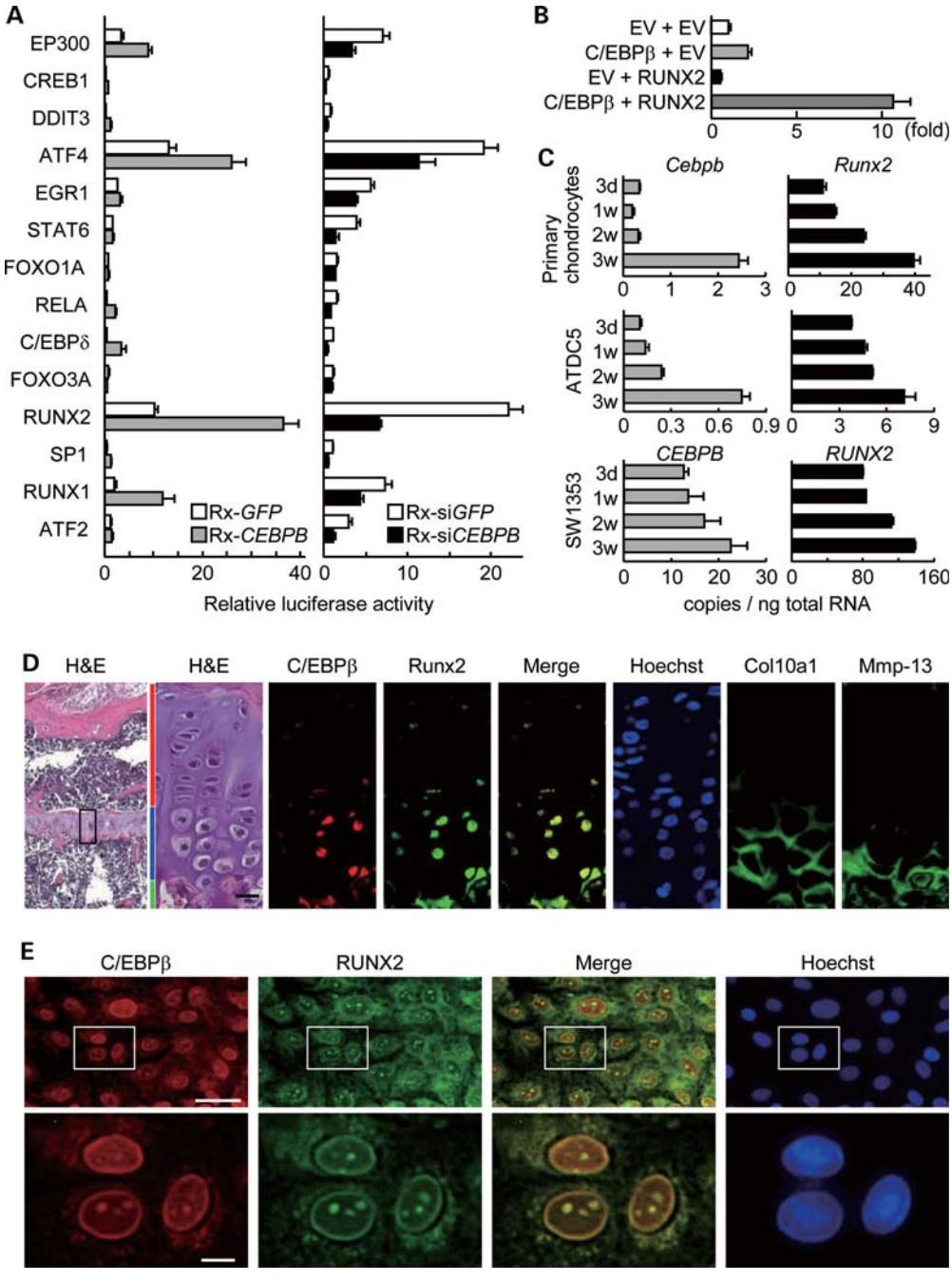

Figure 1. Identification of RUNX2 as a transcriptional partner of C/EBPβ in chondrocytes. (**A**) Luciferase activities after transfections of 14 selected transcription factors into human chondrogenic SW1353 cells with a reporter construct containing three consensus C/EBP-binding sequences, which are retrovirally transfected with *CEBPB* (Rx-*CEBPB*) or the siRNA (Rx-si*CEBPB*), when compared with the respective control (Rx-*GFP* or Rx-si*GFP*). Experiments were done in triplicate with data shown as means ± SEM. (**B**) Mammalian two-hybrid assay by transfections of vectors expressing GAL4–RUNX2 and VP16–C/EBPβ fusion proteins with the luciferase reporter vector with GAL4-binding sites into HeLa cells. Experiments were done in triplicate with data shown as means ± SEM of relative fold increase in luciferase activity when compared with EV + EV (which was arbitrarily set to 1). (**C**) The time course of mRNA levels of *Cebpb* and *Runx2* during differentiation of mouse primary chondrocytes, ATDC5 cells and SW1353 cells cultured for 3 weeks. Experiments were done in triplicate with data shown as means ± SEM. (**D**) Hematoxylin-eosin (H&E) and immunostaining with antibodies to C/EBPβ (red), Runx2 (green), the merged images (yellow), Col10a1, Mmp-13 and Hoechst nuclear staining (blue) in the growth plate cartilage of proximal tibias of 16-week-old mice. The boxed area in the left H&E-stained image indicates the regions shown in the right-enlarged images. Red, blue and green bars indicate layers of proliferative and hypertrophic zones and bone area, respectively. Scale bar, 20 μm. (**E**) Subcellular localization of C/EBPβ (red), RUNX2 (green) and the merged images (yellow) in SW1353 cells. Boxed areas in top images indicate the regions shown in the respective bottom-enlarged images. Scale bars, 50 μm (top) and 10 μm (bottom).

development in surgical and age-related OA models. In a surgical model by inducing instability to the knee joints of 8-week-old mice (4,5), C/EBPβ and Runx2 were co-expressed in chondrocytes of the superficial joint cartilage of wild-type mice with OA development for 8 weeks after surgery (Fig. 3A). To know the functional involvement, we compared

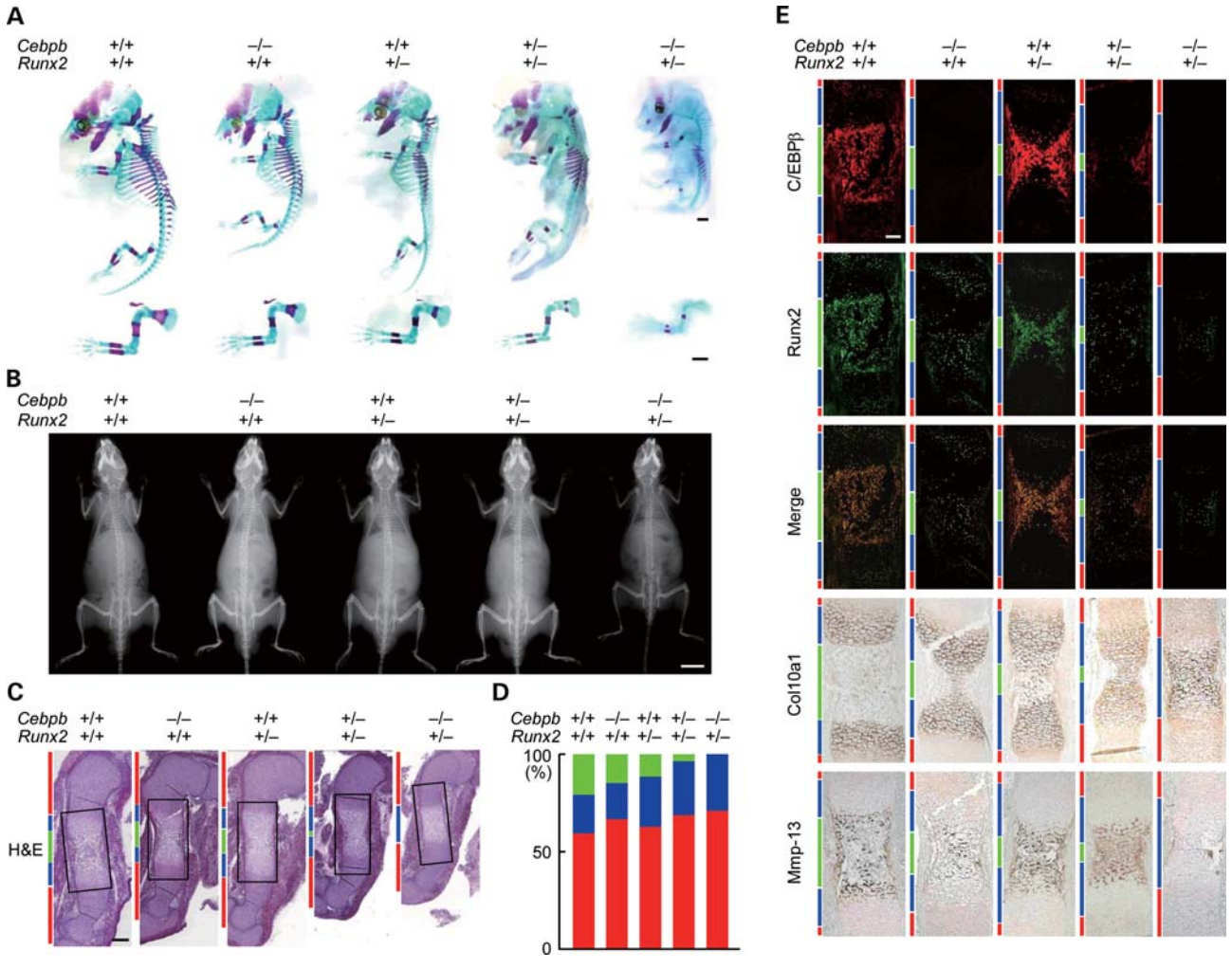

Figure 2. Skeletal findings of five genotype littermates. (**A**) Double staining with Alizarin red and Alcian blue of the whole skeletons (top) and forelimbs and clavicles (bottom) of wild-type (*Cebpb*$^{+/+}$;*Runx2*$^{+/+}$), *Cebpb* homozygous-knockout (*Cebpb*$^{-/-}$), *Runx2* heterozygous-knockout (*Runx2*$^{+/-}$), *Cebpb* heterozygous- and *Runx2* heterozygous-knockout (*Cebpb*$^{+/-}$;*Runx2*$^{+/-}$) and *Cebpb* homozygous- and *Runx2* heterozygous-knockout (*Cebpb*$^{-/-}$;*Runx2*$^{+/-}$) littermates (E14.5). Scale bars, 1 mm. (**B**) Plain radiographs of the whole skeletons of five genotype littermates at 12 weeks of age. Scale bar, 1 cm. (**C**) H&E staining of the humerus of five genotype littermates (E14.5). The boxed areas indicate the regions shown in the enlarged immunostaining images in (**E**). Red, blue and green bars to the left indicate layers of proliferative and hypertrophic zones and bone area, respectively. Scale bar, 200 μm. (**D**) Percentage of the length of proliferative zone (red), hypertrophic zone (blue) and bone area (green) over the total humeral length of the five genotype littermates. (**E**) Immunostaining with antibodies to C/EBPβ (red), Runx2 (green), the merged images (yellow), Col10a1 and Mmp-13 in the boxed areas above. Scale bar, 100 μm.

OA development among wild-type, *Cebpb*$^{+/-}$, *Runx2*$^{+/-}$, and *Cebpb*$^{+/-}$;*Runx2*$^{+/-}$ littermates that did not show significant skeletal abnormality under physiological conditions (Fig. 2B and Supplementary Material, Fig. S5A). We did not use *Cebpb*$^{-/-}$ or *Cebpb*$^{-/-}$;*Runx2*$^{+/-}$ mice in this experiment since their skeletons were originally small, the joint shape was abnormal and the activity was low, so that mechanical stress caused by the joint instability was not assumed to be comparable with that of wild-type mice. The *Cebpb*$^{+/-}$ or *Runx2*$^{+/-}$ mice showed moderate suppression of OA development, as we previously reported (4,11), and the *Cebpb*$^{+/-}$;*Runx2*$^{+/-}$ mice exhibited greater suppression (Fig. 3A), which was confirmed by quantification with the OARSI histopathology grading systems (16,17) (Fig. 3B). When compared with knockout of either one allele of *Cebpb* or *Runx2*, the compound insufficiency caused a considerable decrease in Mmp-13, but not Col10a1, Mmp-9, Adamts4, Adamts5 or Vegf (Fig. 3A and Supplementary Material, Fig. S5B). Here again, Mmp-3 expression was similarly decreased in the *Cebpb*$^{+/-}$;*Runx2*$^{+/-}$ and *Cebpb*$^{+/-}$ cartilages, suggesting the effect of deficiency of one allele of *Cebpb* (Supplementary Material, Fig. S5B). In an age-related OA model using 1-year-old mice of four genotypes under physiological conditions, knockout of either one allele of *Cebpb* or *Runx2* also caused moderate suppression of OA development and the compound insufficiency caused greater and significant suppression with a decrease in Mmp-13 expression (Fig. 3C and D).

In surgical human knee joint specimens, C/EBPβ and RUNX2 were co-expressed in the tibial cartilage with severe degradation (modified Mankin score = 13), although little detected in that with mild degradation (modified Mankin score = 4) (Fig. 3E and Supplementary Material, Fig. S5C).

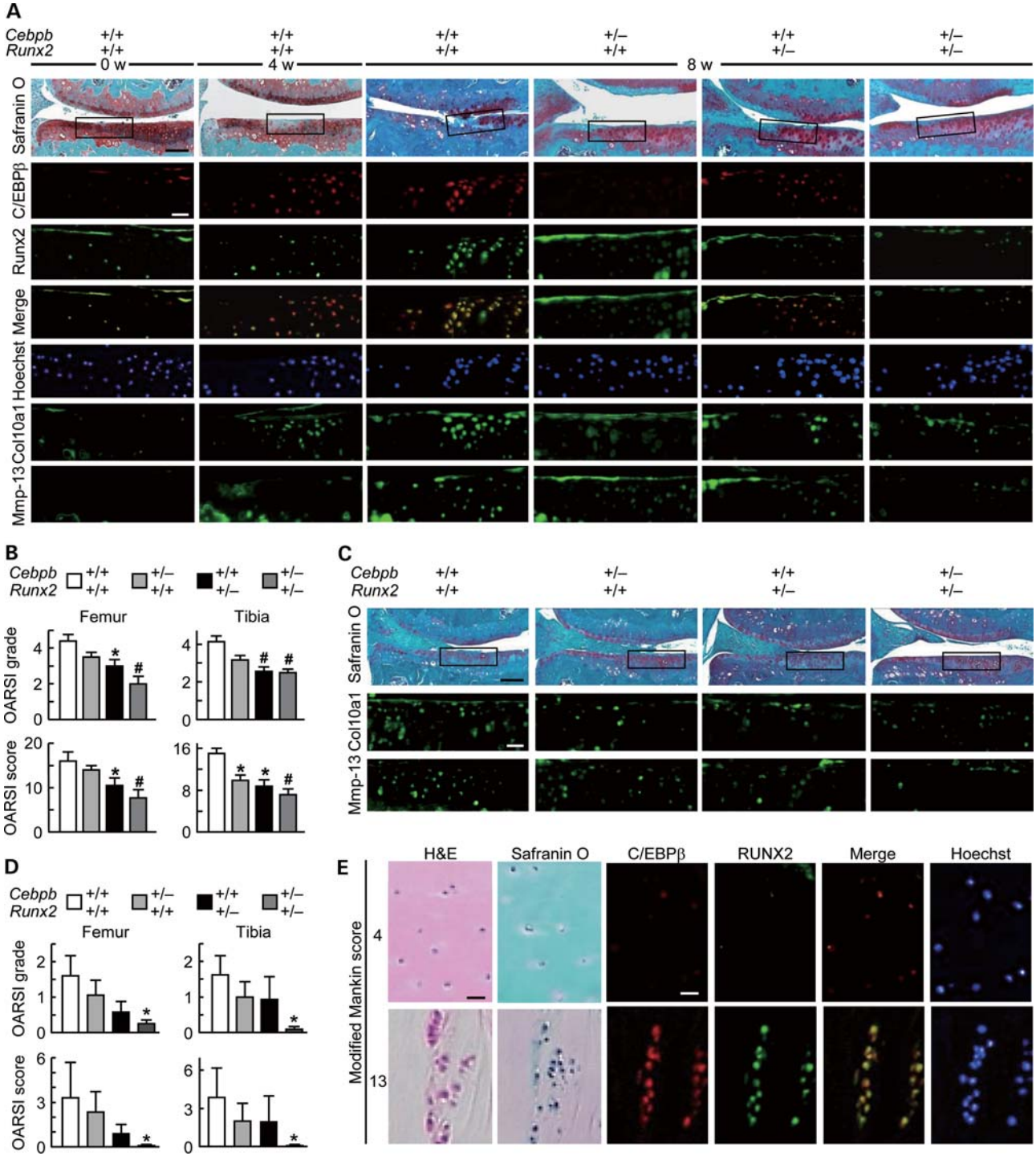

Figure 3. Contribution of C/EBPβ and RUNX2 to OA development. (**A**) Safranin O staining and immunostaining with antibodies to C/EBPβ (red), Runx2 (green), the merged images (yellow), Col10a1, Mmp-13 and Hoechst nuclear staining of joint cartilage 0–8 weeks after surgical OA induction in the knee joints of 8-week-old wild-type (+/+), *Cebpb*$^{+/-}$, *Runx2*$^{+/-}$ and *Cebpb*$^{+/-}$;*Runx2*$^{+/-}$ littermates. Boxed areas in each Safranin O-stained image indicate the regions shown in the enlarged immunofluorescent images below. Scale bars, 200 μm (top) and 100 μm (bottom). (**B**) Quantification of OA development on the femoral and tibial cartilage by OARSI histopathology grading systems in the knee joints of the four genotypes above. Data are expressed as means ± SEM. $n = 8$, $^{*}P < 0.05$ and $\#P < 0.01$ versus wild-type. (**C**) Safranin O staining and immunostaining with antibodies to Col10a1 and Mmp-13 in the knee joints of 1-year-old littermates of four genotypes. Boxed areas in each Safranin O-stained image indicate the regions shown in the enlarged immunofluorescent images below. Scale bars, 200 μm (top) and 100 μm (bottom). (**D**) Quantification of OA development as above in 1-year-old. $n = 8$, $^{*}P < 0.05$ versus wild-type. (**E**) H&E staining, Safranin O staining and immunostaining with antibodies to C/EBPβ (red), RUNX2 (green) and the merged images (yellow) in human tibial cartilages of mild (modified Mankin score = 4) and severe degradation (13) stages obtained as surgical specimens of total knee arthroplasty. Scale bars, 50 μm.

Table 1. Association of polymorphisms in the CEBPB locus with knee OA in a Japanese population of the ROAD study

SNP	Allele [1/2]	Knee OA [11]	[12]	[22]	Control [11]	[12]	[22]	MAF Knee OA	Control	Test for allele frequency[a] *P* value	OR (95%CI)
rs35698361	[GC/TT]	106	68	14	129	91	12	0.255	0.248	0.803	1.04 (0.76–1.42)
rs4253439	[C/T]	91	74	23	96	101	35	0.319	0.369	0.134	0.80 (0.60–1.07)

MAF, minor allele frequency; OR, odds ratio; CI, confidence interval.
[a]Pearson's χ^2-test.

To further investigate a possible association of the *CEBPB* gene with knee OA in humans, we searched a Japanese population-based cohort of the ROAD study (18) for sequence variations in the exon and the 5′-end flanking region of the *CEBPB* gene and identified two polymorphisms with minor allele frequencies >0.1: rs35698361 (GC and TT for major and minor alleles, respectively, at −422 to − 421 from transcription start site (TSS); minor allele frequency = 0.251) and rs4253439 (C and T for major and minor alleles, respectively, at +636 from TSS; minor allele frequency = 0.346) (Table 1 and Supplementary Material, Fig. S6). However, a case-control comparison of allelic frequencies and their haplotype frequencies between 188 subjects with knee OA and 232 controls showed no significant association of these polymorphisms with knee OA ($P > 0.05$), implicating that C/EBPβ may not regulate human OA development by its own gene level.

C/EBPβ and RUNX2 transactivate MMP-13 as a protein complex in chondrocytes

To examine the downstream target of C/EBPβ and RUNX2 in chondrocytes, we created stable lines of SW1353 cells with retroviral overexpression of *CEBPB, RUNX2,* or their combination. *COL10A1* and *MMPs* as well as alkaline phosphatase (ALP) staining, but not *ADAMTSs* or *VEGFA*, were induced by *CEBPB* or *RUNX2* overexpression, and the induction of *MMP13* alone was significantly enhanced by the combination as compared to the single overexpression (Fig. 4A). Although cell proliferation was inhibited by the single overexpression of *CEBPB* or *RUNX2*, as we reported previously (11), this was not enhanced by their combination (Fig. 4B). In addition to endogenous expression, we examined the promoter activity of these genes by the luciferase assay, and confirmed the enhancement of the *MMP13* transactivation by the combination (Fig. 4C). For the loss-of-function analysis, we have created stable lines of SW1353 cells with retroviral overexpression of specific siRNAs for *CEBPB, RUNX2* or their combination, and found that the compound knockdown caused significant suppression of *COL10A1, MMPs, ADAMTS4, VEGFA,* and *ALP* (Fig. 4D). These lines of evidence indicate that C/EBPβ and RUNX2 may cooperatively promote cartilage degradation during the skeletal growth and OA development mainly through stimulation of the MMP-13 expression.

We further examined the mechanism underlying the transactivation of *MMP13* by the combination of *CEBPB* and *RUNX2*. Deletion analyses of the 1 kb fragment of the *MMP13* promoter predicted the core responsive element to be located between −144 and −89 bp (Fig. 5A), which contains a C/EBP-binding motif (−103/−97) and a RUNX-binding motif (osteoblast-specific *cis*-acting element 2 [OSE2]; −138/−132). Site-directed mutagenesis in each motif caused significant suppression of the promoter activation by C/EBPβ and RUNX2, respectively, and that in both motifs caused further suppression of the activation by RUNX2, C/EBPβ, and their combination (Fig. 5B). Electrophoretic mobility shift assay (EMSA) showed the binding of C/EBPβ and RUNX2 proteins with the oligonucleotide including the region containing C/EBP and OSE2 motifs (Fig. 5C). The binding of C/EBPβ or RUNX2 was blocked only when mutations were created in both motifs, but not by mutagenesis in either motif alone, suggesting that these factors bind to respective motifs as a protein complex. The specificity was verified by the cold competition. Additionally, the supershift with C/EBPβ or RUNX2 antibody showed the specific binding of C/EBPβ or RUNX2 protein to the respective motifs. The chromatin immunoprecipitation (ChIP) assay showed the *in vivo* binding of C/EBPβ and RUNX2 to this region (Fig. 5D, top and middle blottings). Furthermore, the ChIP assay followed by release of the immune complexes and reimmunoprecipitation (ChIP-reIP assay) showed that the immunoprecipitate with a RUNX2 antibody was further immunoprecipitated by a C/EBPβ antibody and amplified by a primer set spanning the binding region (Fig. 5D, extreme right lane of the bottom blotting, and E, extreme right graph), confirming the complex formation of C/EBPβ and RUNX2 on this region. However, our sequence analyses using knee OA subjects in the ROAD study failed to detect genetic variations around this binding region in the human *MMP13* promoter (Fig. 5F), again implicating that human OA may not be regulated by the gene level of the region.

Hypoxia-inducible factor-2α (HIF-2α) is a transcriptional inducer of C/EBPβ in chondrocytes

Finally, to identify the upstream mechanism that regulates C/EBPβ expression, we performed a screening of transcription factors using a human *CEBPB* promoter fragment (−740 to +65 bp) (Fig. 6A). Among candidate molecules that are known to regulate chondrocyte differentiation, such as sex-determining region Y box (SOX), RUNX, myocyte enhancer factor-2C (MEF2C), v-rel reticuloendotheliosis viral oncogene homolog A (RELA), HIF, other C/EBPs, ATF, specificity protein-1 (SP1), intercellular domain of Notch1 (Notch1-ICD), recombination signal-binding protein for immunoglobulin kappa J region (RBP-J) and hairy and enhancer of split 1 (HES1), we found that HIF-2α (encoded by *EPAS1*) showed the strongest activation. Deletion analyses predicted the core responsive element to be located between −103 and −46 bp

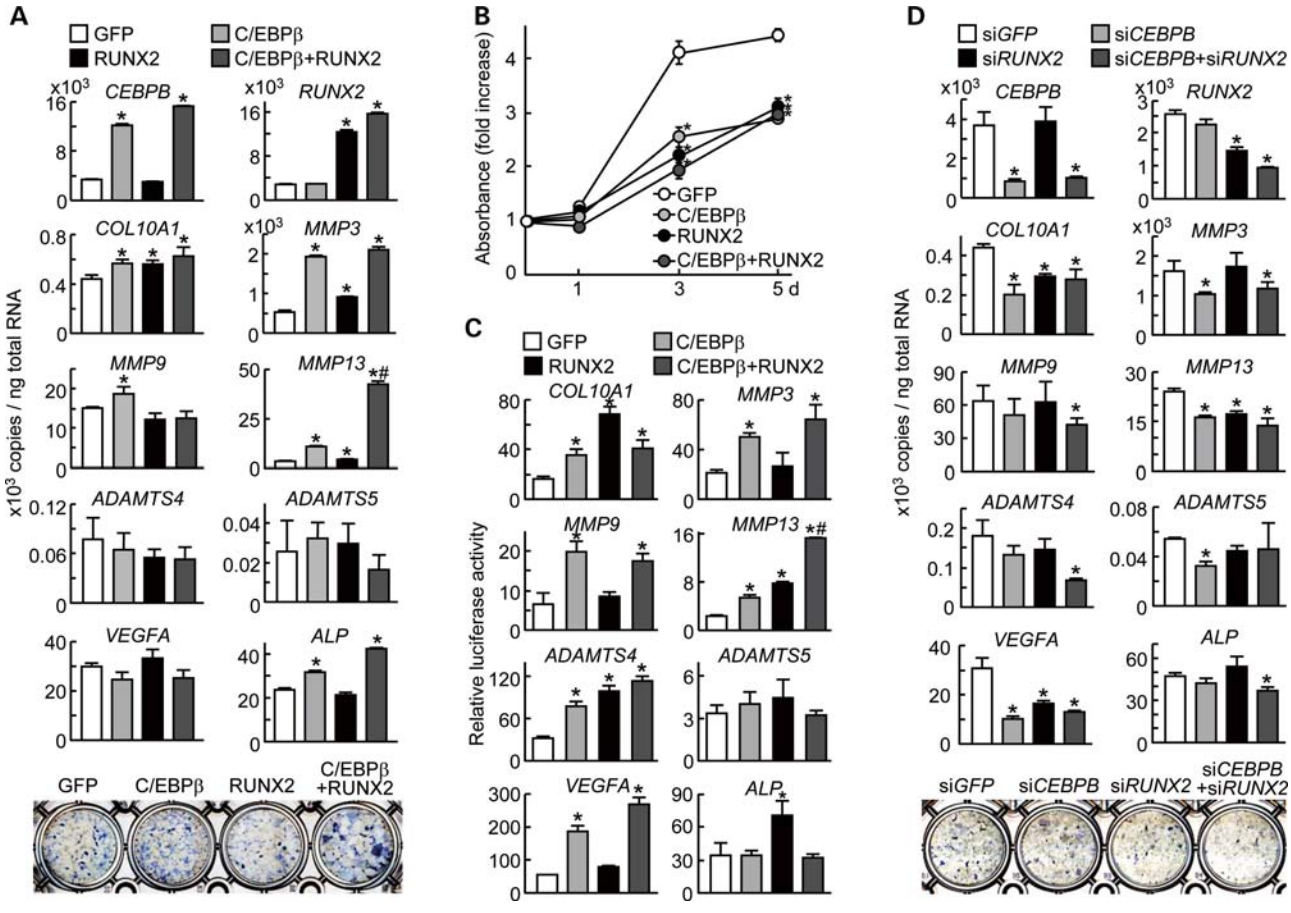

Figure 4. Effects of gain and loss of functions of C/EBPβ and RUNX2 on endochondral ossification parameters in cultures of chondrocytes. (**A**) mRNA levels of *CEBPB*, *RUNX2*, *COL10A1, MMP3*, *9*, *13*, *ADAMTS4*, *5*, *VEGFA* and *ALP* (graphs) and ALP staining (bottom) in stable lines of SW1353 cells retrovirally transfected with *CEBPB, RUNX2*, their combination, or the control *GFP*. (**B**) Growth curves by the CCK-8 assay of stable lines of SW1353 cells retrovirally transfected with the genes above. $^{*}P < 0.01$ versus *GFP* (**C**) Promoter activities by luciferase assays of *COL10A1, MMP3, 9, 13, ADAMTS4, 5, VEGFA* and *ALP* by transfections of *CEBPB, RUNX2*, their combination or the control *GFP* in SW1353 cells co-transfected with reporter constructs containing respective proximal promoter fragments (∼1–3 kb). (**D**) mRNA levels of the factors above and ALP staining in stable lines of SW1353 cells retrovirally transfected with siRNA specific for *CEBPB, RUNX2,* their combination or the control *GFP*. All experiments were done in triplicate with data shown as means ± SEM. $^{*}P < 0.05$ versus *GFP* or si*GFP*, $^{\#}P < 0.05$ versus both *CEBPB* alone and *RUNX2* alone.

(Fig. 6B), which contains a hypoxia-responsive element (HRE) motif (−69/−61). Site-directed mutagenesis in this motif caused a significant suppression of the promoter activation by HIF-2α (Fig. 6C). EMSA showed the binding of HIF-2α protein with this HRE region in the *CEBPB* promoter, and the complex specificity was confirmed by the cold competition and by the supershift with an antibody to HIF-2α (Fig. 6D). In cultured primary chondrocytes, the *Cebpb* expression was enhanced by retroviral overexpression of HIF-2α and suppressed by that of the dominant-negative mutant (DN-HIF-2α) (Fig. 6E). We then looked at the C/EBPβ expression in the limb cartilage and OA joint cartilage of $Epas1^{+/-}$ mice, since $Epas1^{-/-}$ mice died at the early embryonic stage, as reported previously (7). The *Epas1* haploinsufficiency caused a decrease in C/EBPβ expression in the limb cartilage of embryos (Fig. 6F). Furthermore, as we previously reported (7), the haploinsufficiency caused a resistance to cartilage degradation in the knee joint after surgical OA induction, which was associated with a decrease in C/EBPβ expression in the joint cartilage (Fig. 6G).

DISCUSSION

Although the previous studies have identified C/EBPβ as a potent transcription factor for endochondral ossification, the knockout in mice ($Cebpb^{-/-}$) caused only a mild and transient impairment of the skeletal growth (11,14,15). This was thought to be owing to a compensatory mechanism by other C/EBP family members like C/EBPδ which is the principal partner for heterodimer formation and has the most similar function to C/EBPβ in mesenchymal cells (19,20). However, the C/EBPδ expression was much weaker than C/EBPβ in skeletal tissues, and was not altered in the $Cebpb^{-/-}$ mice (11,21), denying this possibility. Instead, we have identified RUNX2 as the most potent transcriptional partner of C/EBPβ. The compound knockout of *Cebpb* and *Runx2* ($Cebpb^{-/-}$;$Runx2^{+/-}$ and $Cebpb^{+/-}$;$Runx2^{+/-}$) affects cartilage degradation which is known to be the most critical step in the endochondral ossification process (22,23). We show that MMP-13 is the direct transcriptional target of C/EBPβ and RUNX2. Although we were unable to identify

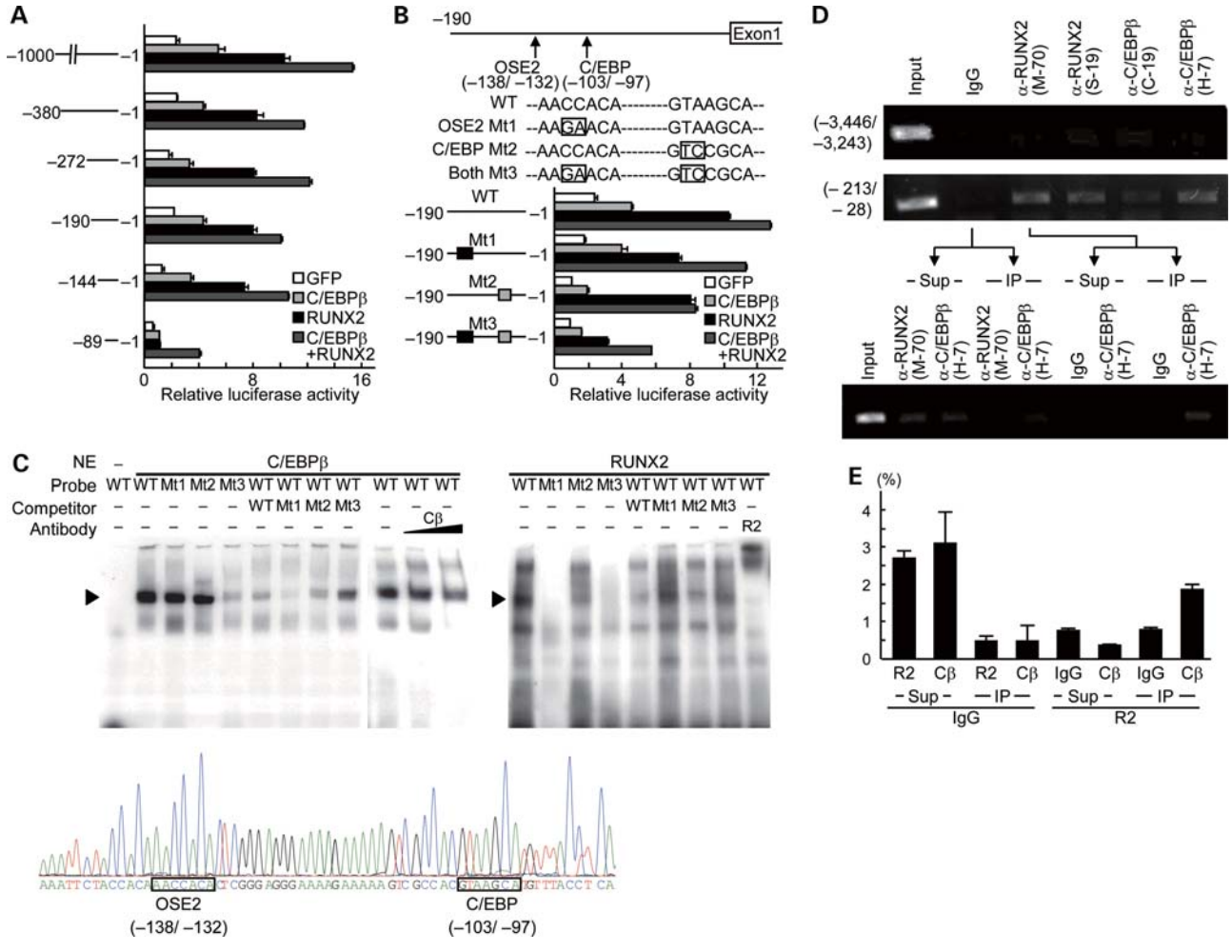

Figure 5. Transcriptional regulation of MMP13 by C/EBPβ and RUNX2. (**A**) Deletion analysis using luciferase-reporter constructs containing the 5′-flanking sequence from −1000 to −1 bp of the *MMP13* gene and a series of deletion fragments in SW1353 cells transfected with *CEBPB, RUNX2*, their combination or the control *GFP*. Experiments were done in triplicate with data shown as means ± SEM. (**B**) Site-directed mutagenesis analysis using luciferase-reporter constructs containing −190/−1 of the *MMP13* gene in the SW1353 cells above. Mutations were created in the OSE2 motif (Mt1), C/EBP-binding motif (Mt2) or both (Mt3). (**C**) EMSA for specific binding (arrowhead) of the wild-type (WT) oligonucleotide probe containing C/EBP and OSE2 motifs above or the mutated probes (Mt1, Mt2 and Mt3) with nuclear extract (NE) of COS-7 cells overexpressing C/EBPβ (left) or RUNX2 (right). The cold competition with a 50-fold excess of unlabeled WT or the mutated probes, and the supershift by an antibody to C/EBPβ (Cβ) or RUNX2 (R2) are presented. (**D**) ChIP (top and middle) and ChIP-reIP (bottom) assays. The ChIP assay was performed using cell lysates of SW1353 cells that were amplified by a primer set spanning the identified region (middle: −213/−28 bp) or not spanning the region (top: −3,446/−3,243 bp) before (input) and after immunoprecipitation with antibodies to RUNX2 (α-RUNX2: M-70 and S-19), C/EBPβ (α-C/EBPβ: C-19 and H-7) or non-immune IgG (IgG). For the ChIP-reIP assay, immunoprecipitates (IP) with non-immune IgG or anti-RUNX2 in the lysates above and their supernatants (Sup) were sequentially applied for another ChIP analysis. (**E**) Quantification of the ChIP-reIP above by the real-time polymerase chain reaction (RT-PCR) analysis using antibodies to C/EBPβ (Cβ), RUNX2 (R2), or non-immune IgG. Experiments were done in triplicate with data shown as means ± SEM of the percentage of the input. (**F**) Sequence analyses around the RUNX2 (OSE2; −138/−132) and C/EBPβ (C/EBP; −103/−97)-binding regions identified by the luciferase assay in the human MMP13 gene of 96 case and control subjects in the ROAD study.

any abnormality of growth plates even in *Cebpb*$^{-/-}$; *Runx2*$^{+/-}$ mice at the age of 16 weeks (Supplementary Material, Fig. S3C), this is not surprising because the growth plates in *Mmp13*$^{-/-}$ mice have a lengthened hypertrophic zone from embryonic stages but the phenotype is gradually ameliorated after birth (23). The *Runx2*$^{-/-}$ mice are known to show a complete lack of Mmp-13 expression in cartilage (24,25), while *Cebpb*$^{-/-}$ mice show the suppression, but not abrogation (Fig. 2E) (11). Furthermore, the C/EBPβ overexpression markedly enhances the MMP-13 expression in combination with RUNX2 (Fig. 4A). These indicate that RUNX2 is indispensable to switch on the *MMP13* transcription, whereas C/EBPβ modulates the MMP-13 expression level in the presence of RUNX2 during the skeletal growth. The insufficient suppression of MMP-13 expression by partial insufficiency of both C/EBPβ and Runx2 in the *Cebpb*$^{+/-}$;*Runx2*$^{+/-}$ limb cartilage (Fig. 2E) and in cultured chondrocytes transfected with the specific siRNAs (Fig. 4D) may be due to the remainder of the basal expression by RUNX2 and its enhancement by C/EBPβ. This insufficient suppression of Mmp-13 expression (Fig. 2E) and more profound effect of impaired transition to hypertrophic differentiation (11) might be the cause of the apparently shortened hypertrophic zone of growth plates in *Cebpb*$^{-/-}$ mice at E14.5 (Fig. 2D). In addition, we could

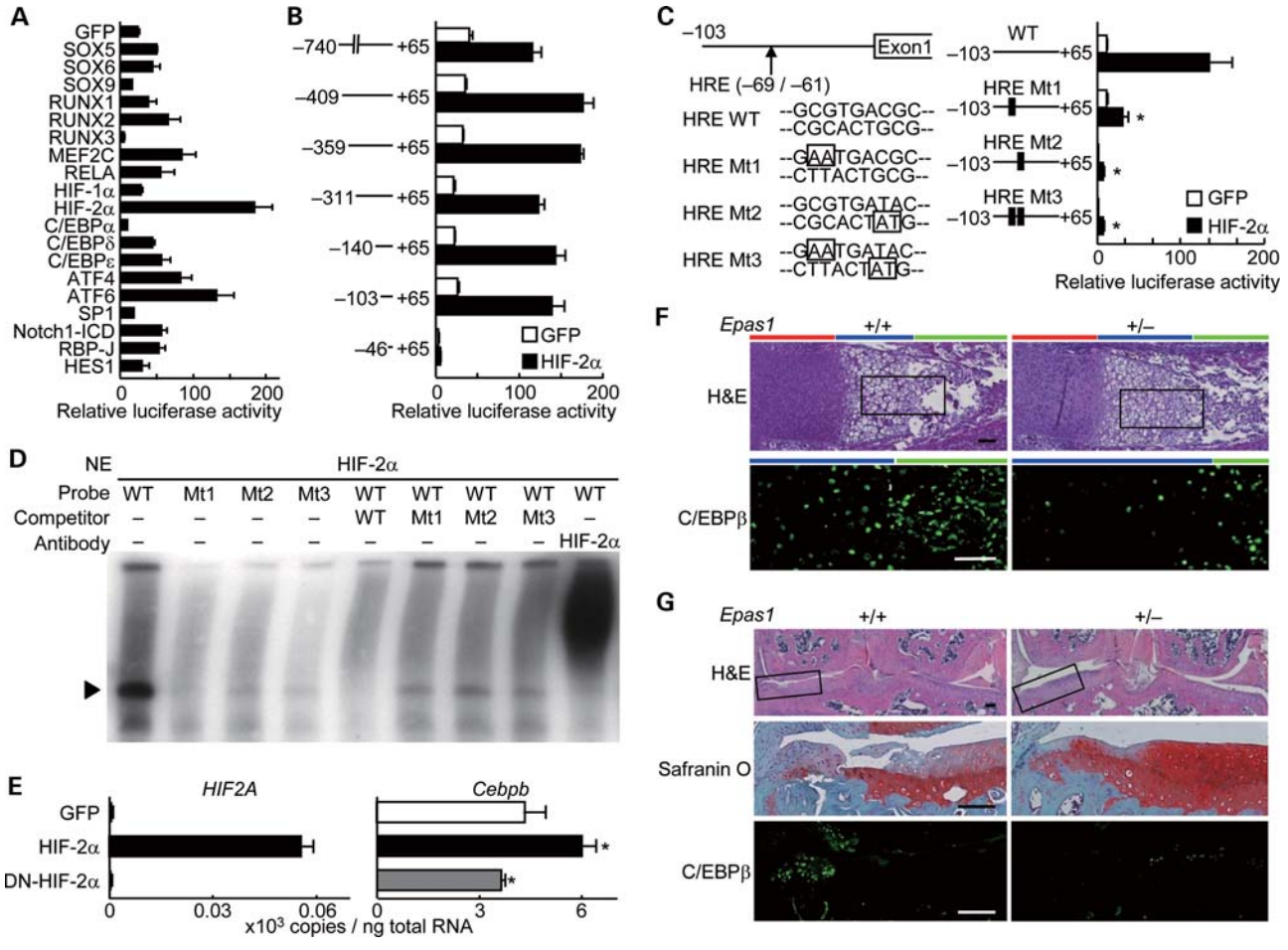

Figure 6. Upstream mechanism that regulates C/EBPβ. (**A**) Luciferase activities after transfection of putative chondrocyte-related transcription factors into SW1353 cells with a reporter construct containing a fragment (−740 to +65 bp) of the *CEBPB* gene. Experiments were done in triplicate with data shown as means ± SEM. (**B**) Deletion analysis using luciferase-reporter constructs containing a series of deletion fragments the *CEBPB* gene in SW1353 cells transfected with HIF-2α or the control GFP. (**C**) Site-directed mutagenesis analysis using luciferase-reporter constructs containing −103/+65 of the *CEBPB* gene with mutations (Mt1, Mt2 and Mt3) in the HRE motif in the cells above. Experiments were done in triplicate with data shown as means ± SEM. $^{*}P < 0.01$ versus wild-type (WT) with HIF-2α. (**D**) EMSA for specific binding (arrowhead) of the WT oligonucleotide probe containing the HRE or the mutated probes above with nuclear extract of COS-7 cells overexpressing HIF-2α. The cold competition with a 50-fold excess of unlabeled WT or the mutated probes, and the supershift by an antibody to HIF-2α are presented. (**E**) mRNA levels of *Cebpb* in mouse primary chondrocytes with retroviral overexpression of HIF-2α, dominant-negative mutant of HIF-2α (DN-HIF-2α), or the control GFP after 1-week cultures. Experiments were done in triplicate with data shown as means ± SEM.$^{*}P < 0.05$ versus GFP. (**F**) H&E staining and C/EBPβ immunostaining in tibial limb cartilages of wild-type (+/+) and *Epas1*$^{+/-}$ littermates (E17.5). Red, blue and green bars indicate layers of proliferative and hypertrophic zones and bone area, respectively. Scale bars, 100 μm. (**G**) H&E, Safranin O stainings and C/EBPβ immunostaining of joints cartilage of +/+ and *Epas1*$^{+/-}$ littermates 8 weeks after surgical OA induction. Scale bars, 100 μm. Boxed areas in each H&E-stained image indicate the regions shown in the enlarged images below.

not deny the possibility that C/EBPβ and RUNX2 have other target molecules, as the *Cebpb*$^{-/-}$;*Runx2*$^{+/-}$ mice exhibited dwarfism even after birth (Fig. 2B), differently from *Mmp13*$^{-/-}$ mice. In fact, the previous studies showed the cooperative regulation of osteocalcin in osteoblasts by C/EBPβ and RUNX2 (14,20), which was supported by our current examination that the phenotype of cleidocranial dysplasia in *Runx2*$^{+/-}$ mice was enhanced under the *Cebpb* insufficiency (Fig. 2A and Supplementary Material, Fig. S2B and C).

The transactivation of *MMP13* by C/EBPβ and RUNX2 is through their specific binding to a C/EBP-binding motif and an OSE2 motif, respectively, in the promoter. Although the identified OSE2 motif is the consensus site for RUNX2 binding in the *MMP13* gene as shown by previous studies (25,26), the identified C/EBP-binding motif is different from that reported in a previous study which predicted a more distal region between −981 bp and −936 bp containing two C/EBP-binding motifs, but not a RUNX-binding motif, in articular chondrocytes of inflammatory arthritis (27). Considering much weaker activation by C/EBPβ alone than in combination with RUNX2 on the 1 kb *MMP13* promoter containing the region (Fig. 4C), and only a slight decrease in the promoter activity between −1000 and −380 bp (Fig. 5A), this distal region may be responsible mainly for MMP-13 expression under inflammatory stimulations like rheumatoid arthritis. According to a crystallization analysis (28), C/EBPβ and RUNX2 are likely to form a complex by binding of basic leucine zipper domain and Runt domain, respectively;

however, there is about 30 bp distance between the C/EBP and OSE2 motifs, suggesting a conformational change of DNA or involvement of intervening proteins. Our screening also identified ATF4 as another possible transcriptional partner of C/EBPβ, but the transactivity on the C/EBP-binding motif was not suppressed by the *CEBPB* knockdown (Fig. 1A). While ATF4 is reported to be a key partner of C/EBPβ in osteoblasts by binding to the OSE1 motif (14), there is no OSE1 motif or other possible binding motif of ATF4 around the identified region in the *MMP13* promoter.

Instead, HIF-2α may possibly function as the intervening protein, since there is an HRE motif (−106/−101) between the C/EBP-binding and OSE2 motifs in this region. This motif is just what we have identified as the core responsive element to HIF-2α in the *MMP13* promoter (7). Also, our present and previous studies have found that HIF-2α directly binds to and activates the promoters of *CEBPB* (Fig. 6) and *RUNX2* (29), indicating that HIF-2α activates the *MMP13* promoter directly and indirectly. HIF-2α is also a potent transactivator of various key factors for the endochondral ossification process: COL10A1, MMP-3, -9, VEGF, Indian hedgehog and parathyroid hormone 1 receptor (7), so that HIF-2α may extensively control the sequential steps of this process. The present human genetic studies have failed to show the association of human *CEBPB* gene polymorphisms with knee OA (Table 1 and Supplementary Material, Fig. S6), nor was there a genetic variation around the identified responsive region in the human *MMP13* promoter (Fig. 5F). In addition, our preliminary genome-wide association studies using the ROAD cohorts have failed to detect a significant association of single nucleotide polymorphisms (SNPs) in the human *RUNX2* gene or in *MMP13* gene with knee OA (data not shown), meaning that C/EBPβ, RUNX2 or MMP-13 may not clinically regulate the OA development by its own gene level. Contrarily, a functional SNP in the human *EPAS1* gene which is related to the promoter activity is associated with knee OA (7). Hence, clinically the genetic variation of HIF-2α might possibly control the expression or activity of C/EBPβ and RUNX2, which then regulates the *MMP13* transactivation during OA development.

Taken together, the present study on a molecular network around C/EBPβ in chondrocytes has identified RUNX2 as the transcriptional partner, MMP-13 as the target and HIF-2α as the inducer during endochondral ossification, implicating that these may possibly represent therapeutic targets of OA. In fact, their knockout mice exhibit resistance to OA development in the experimental models, and transgenic mice overexpressing *Mmp13* in joint cartilage exhibit enhancement of cartilage degradation (4,7,11,30,31). Although ADAMTS5 is known to be another key regulator of OA development in the mouse models (32,33), ADAMTS4 and ADAMTS5 are little regulated by C/EBPβ or RUNX2 (Fig. 4 and Supplementary Material, Figs. S4 and S5B), indicating an independent pathway. The $Cebpb^{+/-}$;$Runx2^{+/-}$ mice show much greater resistance to OA development than $Cebpb^{+/-}$ or $Runx2^{+/-}$ mice in the surgical and age-related models (Fig. 3), and little affected the skeletal growth (Fig. 2). Hence, the C/EBPβ and RUNX2 complex may represent a rational therapeutic target for OA with minimal effects on physiological skeletal homeostasis. Establishment of an effective and selective delivery system to chondrocytes, or identification of related extracellular signals that might be easier to target will be the next task to realize a disease-modifying treatment of OA.

MATERIALS AND METHODS

Computational predictions

We used database and online resource STRING ver8.3 (http://string.embl.de/, last accessed on November 24, 2011) generalizing access to protein interaction data, by integrating known and predicted interactions from a variety of sources.

Construction of expression vectors

We prepared expression vectors for the luciferase assay in pCMV-HA (Clontech) and siRNA vectors for the human *CEBPB* and *RUNX2* gene (NM_005194.2: nucleotides 1633–1653, and NM_001024630.3: nucleotides 4311–4331, respectively) in piGENEhU6 vectors (iGENE Therapeutics). We created the dominant-negative HIF-2α mutant as described previously (34). We generated retroviral vectors using pMx vectors as described previously (35) and adenovirus vectors by the AdenoX Expression system (Clontech), and we verified all vectors by DNA sequencing.

Mice

Cebpb- and *Runx2*-mutant mice were gifts from Shizuo Akira (Osaka University) and Toshihisa Komori (Nagasaki University), respectively (36,37). We purchased *Epas1*-mutant mice (38) from the Jackson Laboratory. We performed all experiments according to the protocol approved by the Animal Care and Use Committee of the University of Tokyo. In each experiment, we compared genotypes of male littermates that were maintained in a C57BL/6 background.

Cell cultures

We cultured SW1353 cells (American Type Culture Collection) and ATDC5 cells (Riken BRC) in Dulbecco's modified Eagle medium: nutrient mixture F-12 (DMEM/F12) (1:1) with 10 and 5% fetal bovine serum (FBS), respectively. We cultured ATDC5 cells for 3 weeks with insulin to induce hypertrophic differentiation. We isolated primary chondrocytes from the ribs of mouse embryos, and cultured them in a monolayer for 1 week in DMEM with 10% FBS. We assessed cell proliferation using a CCK-8 Assay Kit (Dojindo) and ALP activity as previously described (11). For immunocytochemistry, after fixation of 3.7% formalin, we incubated the cells with antibodies to C/EBPβ (C-19; Santa Cruz Biotechnology Inc.), RUNX2 (27-K; ibid). We used a secondary antibody conjugated with Alexa Fluor 568 (Invitrogen) for C/EBPβ, and a CSA II Biotin-Free Catalyzed Amplification System (DAKO) for RUNX2, and applied Hoechst 33258 nuclear stain (Invitrogen) for counterstaining.

Mammalian two-hybrid assay

We performed the mammalian two-hybrid assay using the Checkmate mammalian two-hybrid system (Promega) and the PicaGene Dual SeaPansy Luminescence Kit (Toyo Ink).

Luciferase assay

We purchased pC/EBP-Luc construct from Stratagene. We prepared the *COL10A1* promoter region (from −1,028 to +127 bp relative to the TSS), *MMP3* (−1551 to +39), *MMP9* (−1775 to +17), *MMP13* (−1000 to −1), *ADAMTS4* (−2406 to +27), *ADAMTS5* (−1242 to +27), *VEGFA* (−1000 to −1), *ALP* (−3000 to +3000) and *CEBPB* (−740 to +65) by polymerase chain reaction (PCR) using human genomic DNA as the template, and we cloned them into the pGL3-Basic vector or pGL4.10 [luc2] vector (Promega). We created deletion and mutation constructs by PCR, performed luciferase assays with the PicaGene Dual SeaPansy Luminescence Kit (Toyo Ink) and showed the data as the ratio of the firefly activities to the *Renilla* activities.

Histological analysis

We performed double staining of skeletons of mouse embryos or neonates with a solution containing Alizarin red S and Alcian blue 8GX (Sigma) after fixation in 99.5% ethanol and acetone. We performed H&E and Safranin O stainings according to standard protocols after fixation in 4% paraformaldehyde buffered with PBS. For immunohistochemistry, we incubated the sections with antibodies to C/EBPβ (C-19; Santa Cruz Biotechnology Inc.), Runx2 (27-K; Santa Cruz Biotechnology Inc.), Vegf (A-20; Santa Cruz Biotechnology Inc.), Mmp-3 (AA07; Santa Cruz Biotechnology Inc.), Mmp-9 (H-129; Santa Cruz Biotechnology Inc.), Adamts4 (H-74; Santa Cruz Biotechnology Inc.) and Adamts5 (H-200; Santa Cruz Biotechnology Inc.), Col10a1 (LSL) and Mmp-13 (Chemicon) diluted 1:500 in blocking reagent. For immunofluorescence, we used a secondary antibody conjugated with Alexa Fluor 568 (Invitrogen) for C/EBPβ, and a CSA II Biotin-Free Catalyzed Amplification System (DAKO) for other molecules, and applied Hoechst 33258 nuclear stain (Invitrogen) for counterstaining. For immunoperoxidase methods in Col10a1 and Mmp-13 detection, we also used the CSAII System, and applied methylgreen for counterstaining. Images of the sections were taken at room temperature with a BZ-8000 microscope (Keyence) and BZ Viewer software (ibid) by using a Plan Apo 10x NA 0.45 objective lens (Nikon). The contrast of the images was enhanced using BZ Analyzer (Keyence) for better rendering without altering the relationship of the target to the control images.

OA experiment

We performed the surgical procedure to create an experimental OA model on 8-week-old male mice as reported previously (4,5) and we analyzed them 8 weeks after surgery. We also used the age-related OA model on 1-year-old mice bred under physiological conditions. We quantified OA severity by the OARSI histopathology grading system (0–6 for grade and 0–24 for score) (16,17), which was assessed by a single observer who was blinded to the experimental group.

Real-time RT–PCR

We extracted total RNA from SW1353 cells cultured for 2 weeks after confluency using standard protocols. We performed real-time RT–PCR with an ABI Prism 7000 Sequence Detection System (Applied Biosystems) using FastStart Universal SYBR Green Master (Roche) with *GAPDH* as the internal control. We ran all reactions in triplicate. Primer sequence information is available upon request.

Electrophoretic mobility shift assay

We prepared nuclear extracts from COS-7 cells adenovirally transfected with C/EBPβ, RUNX2 or HIF-2α, and we performed the EMSA with the DIG Gel Shift Kit (Roche). Regions of the oligonucleotide probe were as follows: *MMP13*, from −150 to −90 bp relative to the TSS; *CEBPB*, −85 to −35. For competition analysis, we used 50-fold excess of unlabeled competitor probe containing the binding reaction. For the supershift experiment, we added 1 μl of an antibody to C/EBPβ (C-19; Santa Cruz Biotechnology Inc.), RUNX2 (M-70; Santa Cruz Biotechnology Inc.) or HIF-2α (H-310; Santa Cruz Biotechnology Inc.).

ChIP and ChIP-reIP assay

We performed the ChIP assay in SW1353 cells with a OneDay ChIP kit (Diagenode). For immunoprecipitation, we used antibodies to RUNX2 (M-70 and S-19; Santa Cruz Biotechnology Inc.), C/EBPβ (C-19 and H-7; Santa Cruz Biotechnology Inc.) and the normal rabbit immunoglobulin G (IgG) (Diagenode). Primer sets, one spanning and the other not spanning the identified responsive element, are ranged from −213 to −28 and from −3446 to −3243, respectively. We further performed the ChIP-reIP assay by the sequential application of the abovementioned ChIP assay analysis on immunoprecipitates with the normal rabbit IgG or anti-RUNX2 in the cell lysates and their supernatants. For the quantification, we performed real-time PCR with the ABI Prism 7000 Sequence Detection System (Applied Biosystems) as the abovementioned.

Human samples

We obtained human samples from individuals undergoing total knee arthroplasty after obtaining written informed consent as approved by the Ethics Committee of the University of Tokyo. We histologically assessed cartilage samples by the modified Mankin scoring system (39,40).

Human genetic studies

We recruited individuals over 50 years of age with ($n = 188$; mean age, 76.9; range, 59–88) and without ($n = 232$; 76.4; 62–87) knee OA in a population-based cohort of the ROAD study (18). We diagnosed OA on the basis of radiographic findings by the Kellgren–Lawrence grading system (41): the knee OA population included individuals with Grades 3 and

4 and the control population with Grades 0 and 1. After obtaining written informed consent as approved by the Ethics Committee, we extracted genomic DNA from peripheral blood leukocytes of individuals using standard protocols. We searched polymorphisms around the *CEBPB* gene using the dbSNP-database (http://www.ncbi.nlm.nih.gov/SNP/, last accessed on November 24, 2011), and we genotyped an identified MNP (rs35698361) by direct DNA sequencing using a sequence primer ranging from −607 to −588 bp relative to the TSS, and the other identified SNP (rs4253439) by PCR-restriction fragment length polymorphism using *BmgT120I* (Takara Bio) as the enzyme. We also genotyped the region around the identified C/EBP-β and RUNX2 binding sites in the human *MMP13* promoter of 96 case and control subjects randomly selected from the ROAD study by direct DNA sequencing using a reverse sequence primer ranging from −48 to −29 bp relative to the TSS. We confirmed that the *P* value of the Hardy–Weinberg equilibrium test in the control population was >0.01.

Statistical analysis

We reported all data as means ± SEM of at least three independent experiments, each performed in triplicate. We compared means of groups by ANOVA, and determined the significance of differences by post-hoc testing using Tukey's method in parametric values and Steel's method in non-parametric values. In the case control association study, we evaluated genotypic and allelic models by the χ^2 test for the Hardy–Weinberg equilibrium using spreadsheet software (Excel). *P* values <0.05 were considered significant.

SUPPLEMENTARY MATERIAL

Supplementary Material is available at *HMG* online.

ACKNOWLEDGEMENTS

We thank H. Asahara for providing a DNA construct. We also thank R. Yamaguchi, H. Kawahara, and K. Yoshikawa for excellent technical assistance.

Conflict of Interest statement. None declared.

FUNDING

This work was supported by grants-in-aid for Scientific Research from the Japanese Ministry of Education, Culture, Sports, Science and Technology [19109007, 21390417, 21591930], by Research Aid from the Japanese Orthopaedic Association; and by the Japan Society for the Promotion of Science (JSPS) through 'Funding Program for World-Leading Innovative R&D on Science and Technology (FIRST program)', initiated by the Council for Science and Technology Policy (CSTP). None of the sponsors had any role in study design, data collection, data analysis, data interpretation or writing of the manuscript.

REFERENCES

1. Kronenberg, H.M. (2003) Developmental regulation of the growth plate. *Nature*, **423**, 332–336.
2. von der Mark, K., Kirsch, T., Nerlich, A., Kuss, A., Weseloh, G., Gluckert, K. and Stoss, H. (1992) Type X collagen synthesis in human osteoarthritic cartilage. Indication of chondrocyte hypertrophy. *Arthritis Rheum.*, **35**, 806–811.
3. Drissi, H., Zuscik, M., Rosier, R. and O'Keefe, R. (2005) Transcriptional regulation of chondrocyte maturation: potential involvement of transcription factors in OA pathogenesis. *Mol. Aspects Med.*, **26**, 169–179.
4. Kamekura, S., Kawasaki, Y., Hoshi, K., Shimoaka, T., Chikuda, H., Maruyama, Z., Komori, T., Sato, S., Takeda, S., Karsenty, G. *et al.* (2006) Contribution of runt-related transcription factor 2 to the pathogenesis of osteoarthritis in mice after induction of knee joint instability. *Arthritis Rheum.*, **54**, 2462–2470.
5. Yamada, T., Kawano, H., Koshizuka, Y., Fukuda, T., Yoshimura, K., Kamekura, S., Saito, T., Ikeda, T., Kawasaki, Y., Azuma, Y. *et al.* (2006) Carminerin contributes to chondrocyte calcification during endochondral ossification. *Nat. Med.*, **12**, 665–670.
6. Kawaguchi, H. (2008) Endochondral ossification signals in cartilage degradation during osteoarthritis progression in experimental mouse models. *Mol. Cells*, **25**, 1–6.
7. Saito, T., Fukai, A., Mabuchi, A., Ikeda, T., Yano, F., Ohba, S., Nishida, N., Akune, T., Yoshimura, N., Nakagawa, T. *et al.* (2010) Transcriptional regulation of endochondral ossification by HIF-2alpha during skeletal growth and osteoarthritis development. *Nat. Med.*, **16**, 678–686.
8. Karsenty, G. and Wagner, E.F. (2002) Reaching a genetic and molecular understanding of skeletal development. *Dev. Cell*, **2**, 389–406.
9. Fosang, A.J., Rogerson, F.M., East, C.J. and Stanton, H. (2008) ADAMTS-5: the story so far. *Eur. Cell. Mater.*, **15**, 11–26.
10. Higashikawa, A., Saito, T., Ikeda, T., Kamekura, S., Kawamura, N., Kan, A., Oshima, Y., Ohba, S., Ogata, N., Takeshita, K. *et al.* (2009) Identification of the core element responsive to runt-related transcription factor 2 in the promoter of human type X collagen gene. *Arthritis Rheum.*, **60**, 166–178.
11. Hirata, M., Kugimiya, F., Fukai, A., Ohba, S., Kawamura, N., Ogasawara, T., Kawasaki, Y., Saito, T., Yano, F., Ikeda, T. *et al.* (2009) C/EBPβ promotes transition from proliferation to hypertrophic differentiation of chondrocytes through transactivation of p57. *PLoS ONE*, **4**, e4543.
12. Johnson, P.F. (2005) Molecular stop signs: regulation of cell-cycle arrest by C/EBP transcription factors. *J. Cell Sci.*, **118**, 2545–2555.
13. Nerlov, C. (2007) The C/EBP family of transcription factors: a paradigm for interaction between gene expression and proliferation control. *Trends Cell Biol.*, **17**, 318–324.
14. Tominaga, H., Maeda, S., Hayashi, M., Takeda, S., Akira, S., Komiya, S., Nakamura, T., Akiyama, H. and Imamura, T. (2008) CCAAT/enhancer-binding protein beta promotes osteoblast differentiation by enhancing Runx2 activity with ATF4. *Mol. Biol. Cell*, **19**, 5373–5386.
15. Tsuchimochi, K., Otero, M., Dragomir, C.L., Plumb, D.A., Zerbini, L.F., Libermann, T.A., Marcu, K.B., Komiya, S., Ijiri, K. and Goldring, M.B. (2010) GADD45beta enhances Col10a1 transcription via the MTK1/MKK3/6/p38 axis and activation of C/EBPbeta-TAD4 in terminally differentiating chondrocytes. *J. Biol. Chem.*, **285**, 8395–8407.
16. Pritzker, K.P., Gay, S., Jimenez, S.A., Ostergaard, K., Pelletier, J.P., Revell, P.A., Salter, D. and van den Berg, W.B. (2006) Osteoarthritis cartilage histopathology: grading and staging. *Osteoarthritis Cartilage*, **14**, 13–29.
17. Glasson, S.S., Chambers, M.G., Van Den Berg, W.B. and Little, C.B. (2010) The OARSI histopathology initiative - recommendations for histological assessments of osteoarthritis in the mouse. *Osteoarthritis Cartilage*, **18**(Suppl. 3), S17–S23.
18. Yoshimura, N., Muraki, S., Oka, H., Kawaguchi, H., Nakamura, K. and Akune, T. (2010) Cohort profile: research on Osteoarthritis/Osteoporosis Against Disability study. *Int. J. Epidemiol.*, **39**, 988–995.
19. Darlington, G.J., Ross, S.E. and MacDougald, O.A. (1998) The role of C/EBP genes in adipocyte differentiation. *J. Biol. Chem.*, **273**, 30057–30060.
20. Gutierrez, S., Javed, A., Tennant, D.K., van Rees, M., Montecino, M., Stein, G.S., Stein, J.L. and Lian, J.B. (2002) CCAAT/enhancer-binding proteins (C/EBP) beta and delta activate osteocalcin gene transcription

and synergize with Runx2 at the C/EBP element to regulate bone-specific expression. *J. Biol. Chem.*, **277**, 1316–1323.
21. Shirakawa, K., Maeda, S., Gotoh, T., Hayashi, M., Shinomiya, K., Ehata, S., Nishimura, R., Mori, M., Onozaki, K., Hayashi, H. *et al.* (2006) CCAAT/enhancer-binding protein homologous protein (CHOP) regulates osteoblast differentiation. *Mol. Cell. Biol.*, **26**, 6105–6116.
22. Ortega, N., Behonick, D., Stickens, D. and Werb, Z. (2003) How proteases regulate bone morphogenesis. *Ann. N. Y. Acad. Sci.*, **995**, 109–116.
23. Stickens, D., Behonick, D.J., Ortega, N., Heyer, B., Hartenstein, B., Yu, Y., Fosang, A.J., Schorpp-Kistner, M., Angel, P. and Werb, Z. (2004) Altered endochondral bone development in matrix metalloproteinase 13-deficient mice. *Development*, **131**, 5883–5895.
24. Inada, M., Yasui, T., Nomura, S., Miyake, S., Deguchi, K., Himeno, M., Sato, M., Yamagiwa, H., Kimura, T., Yasui, N. *et al.* (1999) Maturational disturbance of chondrocytes in Cbfa1-deficient mice. *Dev. Dyn.*, **214**, 279–290.
25. Jimenez, M.J., Balbin, M., Lopez, J.M., Alvarez, J., Komori, T. and Lopez-Otin, C. (1999) Collagenase 3 is a target of Cbfa1, a transcription factor of the runt gene family involved in bone formation. *Mol. Cell. Biol.*, **19**, 4431–4442.
26. Selvamurugan, N., Jefcoat, S.C., Kwok, S., Kowalewski, R., Tamasi, J.A. and Partridge, N.C. (2006) Overexpression of Runx2 directed by the matrix metalloproteinase-13 promoter containing the AP-1 and Runx/RD/Cbfa sites alters bone remodeling *in vivo*. *J. Cell. Biochem.*, **99**, 545–557.
27. Hayashida, M., Okazaki, K., Fukushi, J., Sakamoto, A. and Iwamoto, Y. (2009) CCAAT/enhancer binding protein beta mediates expression of matrix metalloproteinase 13 in human articular chondrocytes in inflammatory arthritis. *Arthritis Rheum.*, **60**, 708–716.
28. Tahirov, T.H., Inoue-Bungo, T., Sasaki, M., Shiina, M., Kimura, K., Sato, K., Kumasaka, T., Yamamoto, M., Kamiya, N. and Ogata, K. (2001) Crystallization and preliminary X-ray analyses of quaternary, ternary and binary protein-DNA complexes with involvement of AML1/Runx-1/CBFalpha Runt domain, CBFbeta and the C/EBPbeta bZip region. *Acta Crystallogr. D Biol. Crystallogr.*, **57**, 850–853.
29. Tamiya, H., Ikeda, T., Jeong, J.H., Saito, T., Yano, F., Jung, Y.K., Ohba, S., Kawaguchi, H., Chung, U.I. and Choi, J.Y. (2008) Analysis of the Runx2 promoter in osseous and non-osseous cells and identification of HIF2A as a potent transcription activator. *Gene*, **416**, 53–60.
30. Little, C.B., Barai, A., Burkhardt, D., Smith, S.M., Fosang, A.J., Werb, Z., Shah, M. and Thompson, E.W. (2009) Matrix metalloproteinase 13-deficient mice are resistant to osteoarthritic cartilage erosion but not chondrocyte hypertrophy or osteophyte development. *Arthritis Rheum.*, **60**, 3723–3733.
31. Neuhold, L.A., Killar, L., Zhao, W., Sung, M.L., Warner, L., Kulik, J., Turner, J., Wu, W., Billinghurst, C., Meijers, T. *et al.* (2001) Postnatal expression in hyaline cartilage of constitutively active human collagenase-3 (MMP-13) induces osteoarthritis in mice. *J. Clin. Invest.*, **107**, 35–44.
32. Glasson, S.S., Askew, R., Sheppard, B., Carito, B., Blanchet, T., Ma, H.L., Flannery, C.R., Peluso, D., Kanki, K., Yang, Z. *et al.* (2005) Deletion of active ADAMTS5 prevents cartilage degradation in a murine model of osteoarthritis. *Nature*, **434**, 644–648.
33. Stanton, H., Rogerson, F.M., East, C.J., Golub, S.B., Lawlor, K.E., Meeker, C.T., Little, C.B., Last, K., Farmer, P.J., Campbell, I.K. *et al.* (2005) ADAMTS5 is the major aggrecanase in mouse cartilage *in vivo* and *in vitro*. *Nature*, **434**, 648–652.
34. Maemura, K., Hsieh, C.M., Jain, M.K., Fukumoto, S., Layne, M.D., Liu, Y., Kourembanas, S., Yet, S.F., Perrella, M.A. and Lee, M.E. (1999) Generation of a dominant-negative mutant of endothelial PAS domain protein 1 by deletion of a potent C-terminal transactivation domain. *J. Biol. Chem.*, **274**, 31565–31570.
35. Kitamura, T. (1998) New experimental approaches in retrovirus-mediated expression screening. *Int. J. Hematol.*, **67**, 351–359.
36. Tanaka, T., Akira, S., Yoshida, K., Umemoto, M., Yoneda, Y., Shirafuji, N., Fujiwara, H., Suematsu, S., Yoshida, N. and Kishimoto, T. (1995) Targeted disruption of the NF-IL6 gene discloses its essential role in bacteria killing and tumor cytotoxicity by macrophages. *Cell*, **80**, 353–361.
37. Komori, T., Yagi, H., Nomura, S., Yamaguchi, A., Sasaki, K., Deguchi, K., Shimizu, Y., Bronson, R.T., Gao, Y.H., Inada, M. *et al.* (1997) Targeted disruption of Cbfa1 results in a complete lack of bone formation owing to maturational arrest of osteoblasts. *Cell*, **89**, 755–764.
38. Tian, H., Hammer, R.E., Matsumoto, A.M., Russell, D.W. and McKnight, S.L. (1998) The hypoxia-responsive transcription factor EPAS1 is essential for catecholamine homeostasis and protection against heart failure during embryonic development. *Genes Dev.*, **12**, 3320–3324.
39. Mankin, H.J., Dorfman, H., Lippiello, L. and Zarins, A. (1971) Biochemical and metabolic abnormalities in articular cartilage from osteo-arthritic human hips. II. Correlation of morphology with biochemical and metabolic data. *J. Bone Joint Surg. Am.*, **53**, 523–537.
40. Ostergaard, K., Andersen, C.B., Petersen, J., Bendtzen, K. and Salter, D.M. (1999) Validity of histopathological grading of articular cartilage from osteoarthritic knee joints. *Ann. Rheum. Dis.*, **58**, 208–213.
41. Kellgren, J.H. and Lawrence, J.S. (1957) Radiological assessment of osteo-arthrosis. *Ann. Rheum. Dis.*, **16**, 494–502.